Applied Catalysis B: Environmental 123–124 (2012) 134–140

Contents lists available at SciVerse ScienceDirect

Applied Catalysis B: Environmental

journal homepage: www.elsevier.com/locate/apcatb

Selective catalytic reduction of NO on single site FeSiBEA zeolite catalyst: Influence of the C_1 and C_2 reducing agents on the catalytic properties

Janusz Janas[a], Wojciech Rojek[a], Tetsuya Shishido[b], Stanislaw Dzwigaj[c,d,*]

[a] Institute of Catalysis and Surface Chemistry, Polish Academy of Sciences, ul. Niezapominajek 8, 30-239, Kraków, Poland
[b] Department of Molecular Engineering, Kyoto University, Kyoto, 615-8510, Japan
[c] UPMC Univ Paris 06, Laboratoire de Réactivité de Surface, Case 178, Site d'Ivry-Le Raphaël, 3 rue Galilée, 94200, Ivry sur Seine, France
[d] CNRS-UMR 7197, Laboratoire de Réactivité de Surface, Case 178, Site d'Ivry-Le Raphaël, 3 rue Galilée, 94200, Ivry sur Seine, France

ARTICLE INFO

Article history:
Received 16 February 2012
Received in revised form 12 April 2012
Accepted 19 April 2012
Available online 25 April 2012

Keywords:
Iron
SiBEA
SCR of NO
Methanol
Methane
Ethanol
Ethylene

ABSTRACT

FeSiBEA zeolite with 0.8 Fe wt% is prepared in acidic condition (pH 2.5) by a two-step postsynthesis method which allows to incorporate iron into framework of zeolite as mononuclear distorted tetrahedral Fe(III) species, as evidenced by XRD, diffuse reflectance UV–vis and X-ray absorption spectroscopy. The single site FeSiBEA catalyst with isolated and framework Fe centres is active in SCR of NO process with C_2 (ethanol and ethylene) reducing agents, with selectivity towards N_2 exceeding 90% in the broad temperature range from 573 to 723 K for maximum NO conversion about 50 and 30% at 573 K for ethanol and ethylene respectively. In contrast, this catalyst is much less active with C_1 (methanol and methane) reducing agents, with maximum selectivity towards N_2 not exceeding 65% with methanol and 10% with methane for maximum NO conversion of 10 and 23% respectively. The low activity in CH_4-SCR of NO on $Fe_{0.8}$SiBEA catalyst containing only isolated mononuclear distorted tetrahedral Fe(III) species in the framework zeolite could be explained by high energy of C—H bond, which should be broken to activate methane molecule.

1. Introduction

Transition metal containing zeolites are active in many catalytic reactions including oxidative dehydrogenation of alkanes [1–3], selective catalytic reduction (SCR) of NO by reducing agents [4–21] and direct N_2O decomposition [22,23]. Iron zeolites are known to be active in several reactions, such as N_2O decomposition [24–27], selective catalytic reduction of NO_x and N_2O [5,28] and selective oxidation of different substrates [29–32]. Although the big number of papers were reported on NO removal since a pioneer works of Iwamoto [33] and Held [34], only in some of their a mechanism of SCR of NO process were deeply discussed and no universal description of this process on zeolites was reported up till now. The main reasons of this were the complexity of various potential active centres in zeolite material and diversity of organic compounds chosen as the NO reducing agents.

The first problem can be greatly reduced if well-defined catalysts with isolated metal centre could be prepared. The current methods of dispersing transition metals in zeolites such as classical impregnation or ion exchange are not efficient method to obtain well defined isolated centre because the presence of iron impurities in commercial zeolites, as we have earlier reported [35]. EPR and Mössbauer spectroscopies have been evidenced that in commercial BEA zeolite iron impurities are present as tetrahedral Fe(III) and octahedral Fe(III) species. Iron impurities present in commercial BEA zeolite are active in the selective catalytic reduction (SCR) of NO by ethanol, with NO conversion higher than 37% and with selectivity towards N_2 higher than 90% in the temperature range 575–775 K. The high activity of commercial BEA suggests that Fe(III) impurities are present in tetrahedral and/or octahedral environments, possibly close to lattice Al, which make them active in the SCR of NO by ethanol. However, this is only an assumption and it should be confirmed. So to prepare well defined Fe single site zeolite catalyst without Fe impurities and Al ions we have developed a two-step postsynthesis method which consists first of creating vacant T-atom sites by removal of Fe impurities and Al ions from framework and extra framework position of BEA zeolite by treatment with nitric acid and then, in the second step, impregnating the resulting pure SiBEA material with Fe precursor [36] to incorporate Fe ions into framework position. As we have recently

* Corresponding author at: UPMC Univ Paris 06, Laboratoire de Réactivité de Surface, Case 178, Site d'Ivry-Le Raphaël, 3 rue Galilée, 94200, Ivry sur Seine, France. Tel.: +33 1 44 27 21 13; fax: +33 1 44 27 60 33.
E-mail address: stanislaw.dzwigaj@upmc.fr (S. Dzwigaj).

0926-3373/$ – see front matter © 2012 Elsevier B.V. All rights reserved.
http://dx.doi.org/10.1016/j.apcatb.2012.04.026

reported [13,37], this postsynthesis method allows, for low Fe content (<2 wt%), to incorporate iron into framework of SiBEA zeolite as isolated distorted tetrahedral Fe(III), without formation of FeO_x oligomers or iron oxide.

In the presented work, the single site FeSiBEA zeolite with 0.8 Fe wt% was prepared containing isolated and framework Fe centres and used as catalyst in SCR of NO with C_1 (methanol and methane) and C_2 (ethanol and ethylene) reducing agents. The choice of alcohols has both application and fundamental purposes, because the lower alcohols are often used as a fuels or additives in different combustion processes and as the reducing agents in SCR of NO process.

The objective of this work was to investigate the influence of the C_1 and C_2 reducing agents on the catalytic properties of FeSiBEA zeolite and to show the role of mononuclear iron species on SCR of NO process.

2. Experimental

2.1. Catalyst preparation

FeSiBEA catalyst with 0.8 Fe wt% was prepared by the two-step postsynthesis method reported earlier [13,36,37]. To obtain the FeSiBEA, 2 g of siliceous beta (SiBEA) zeolite (Si/Al > 1300), obtained by treatment of a tetraethyl ammonium BEA zeolite (Si/Al = 11) provided by RIPP (China) in a 13 mol L^{-1} HNO_3 (supplier: VWR Prolabo, AnalaR Normapur 68%) solution (at 353 K for 4 h, were stirred for 24 h at 298 K in aqueous solution containing 1×10^{-3} mol L^{-1} of $Fe(NO_3)_3 \times 9{\cdot}H_2O$ (supplier: Merck, for analysis, purity > 99%). Then, the suspension was stirred in evaporator under vacuum of a water pump for 2 h at 353 K until the water was completely evaporated. The solid was washed and then dried in air at 353 K for 24 h. The resulting powder-like material was finally pelleted, crushed and sieved. The 0.3–0.6 mm diameter fraction was selected for catalytic experiments. The solid containing 0.8 Fe wt% was labelled $Fe_{0.8}$SiBEA.

2.2. Catalyst characterization

Powder X-ray diffractograms (XRD) were recorded at ambient atmosphere on a Siemens D5000 using the CuKα radiation (λ = 154.05 pm).

Diffuse reflectance UV–vis (DR UV–vis) spectra were recorded at ambient atmosphere on a Cary 5000 Varian spectrometer equipped with a double integrator with polytetrafluoroethylene.

X-ray absorption spectra (XAS) were recorded on the beam line BL01B1 at SPring-8 of JASRI, Japan (Proposal no. 2011A1173). EXAFS spectra were recorded in a transmission mode at room temperature by using two ion chambers (N_2 (I_0) and 85% N_2 diluted with Ar (I)). Si (1 1 1) single crystal was used to obtain a monochromatic X-ray beam. Analysis of EXAFS data was performed using the REX2000 program (Version 2.5.9, Rigaku Corp.). For EXAFS analysis, the oscillation was first extracted from EXAFS data using a spline smoothing method [38]. The oscillation was normalized by the edge height around 70–100 eV above the threshold. Fourier transforms (FT) of k^3-weighted EXAFS spectra were obtained over a k-range of 3.5–14.0 $Å^{-1}$. Fourier transformed data for each peak were analyzed by a curve-fitting method, using theoretical phase shifts and amplitude functions derived from the FEFF8.2 program [39].

2.3. Catalyst activity measurements

The activity of SiBEA and $Fe_{0.8}$SiBEA samples in the SCR of NO with different C_1 (methanol and methane) and C_2 (ethanol and ethylene) reducing agents was measured in a conventional flow reactor coupled to an analytical system. Gas chromatograph (CHROM-5) provided with thermal conductivity detector (TCD) and flame ionization detector (FID) was used for analysis of gas-phase components. CO_2, N_2O and ethylene were separated on packed nickel HayeSep R column and O_2, N_2 and CO were separated on MS 5A column (Supelco). The organic substrates such as nitrocompounds, acetonitrile and acetic aldehyde were separated on packed: 10% SP-1000 on 80/100 Supelcort and 10% SP-2100 on 100/120 Supelcort columns using FID detector. The calculations were done using CHROMA 2000 computer analytical program. The O_2, NO_x and CO concentrations were continuously monitored using GA-60 (MADUR) flue gas analyser provided with electrochemical sensors. The NO and ethylene concentrations were additionally measured by means of Photovac 10S50 GC with KCl-alumina column using photoionization detector. For the calculation of formaldehyde concentration and to check the presence of the active intermediates as the HCN, NH_3, C_1–C_2 oxygenates and nitroalkanes, among the reaction products, the FTIR multichannel GASMET DX-4000 gas analyzer was used.

The composition of the feed was: 1000 ppm NO, 2000 ppm of C_1 (methanol, methane) reducing agents, 1000 ppm of C_2 (ethanol, ethylene) reducing agents, 2 vol.% of O_2 with a bed volume 1 ml (about 20 mm length) and GHSV (gas hourly space velocity) 10,000 h^{-1}. Before catalytic tests, the samples were pretreated up to 523 K in oxygen/helium mixture and then NO and/or organic reducer vapour streams were switched on. The standard conditions were: catalytic runs at 523–773 K (each temperature level for 1 h) and (NO_x and CO_x concentrations at the reactor outlet were continuously monitored for checking if pseudo steady-state conditions were established). In order to check a reproducible activity during the first run the reaction temperature was increased every 50 K intervals from 523 to 773 K, and then catalytic tests were repeated in the same manner but in descending reaction temperatures. In both runs a similar activity of catalyst has been observed for all reducing agents.

All the conversion and selectivity values used in the text were defined and calculated in standard manner and presented in %. Because of the difficulty to determine N_2 concentrations at the reactor outlet, the selectivity towards N_2 was determined as follows:

$$S_{N_2} = 100 - (S_{NO_2} + S_{N_2O} + S_{NH_3} + S_{OrgN}), \quad (\%)$$

where: S_{NO_2} S_{N_2O} and S_{NH_3} are the selectivity towards NO_2, N_2O and NH_3, respectively and S_{OrgN} is the sum of selectivities towards nitrogen-containing organic compounds.

3. Results and discussion

3.1. State of iron in FeSiBEA zeolite

3.1.1. X-ray diffraction

Fig. 1 shows the XRD patterns of AlBEA, SiBEA and $Fe_{0.8}$SiBEA which are all of typical BEA zeolite. This indicates that crystallinity of BEA zeolite is preserved after dealumination and incorporation of Fe ions in zeolite structure. The decrease of the d_{302} spacing related to the narrow main diffraction peak near 22–23° from 3.942 (AlBEA) (with 2θ of 22.55°) to 3.912 Å (SiBEA) (with 2θ of 22.71°) upon dealumination indicates contraction of the matrix as a result of removal Al [36,40]. In contrast, the significant increase to 3.939 Å (with 2θ of 22.64°) upon introduction of 0.8 Fe wt% into SiBEA indicates expansion of the matrix as already reported for VSiBEA zeolites [36,40]. The increase of the d_{302} spacing evidences the incorporation of Fe into the framework of zeolite, in line with previous report on BEA zeolite [41].

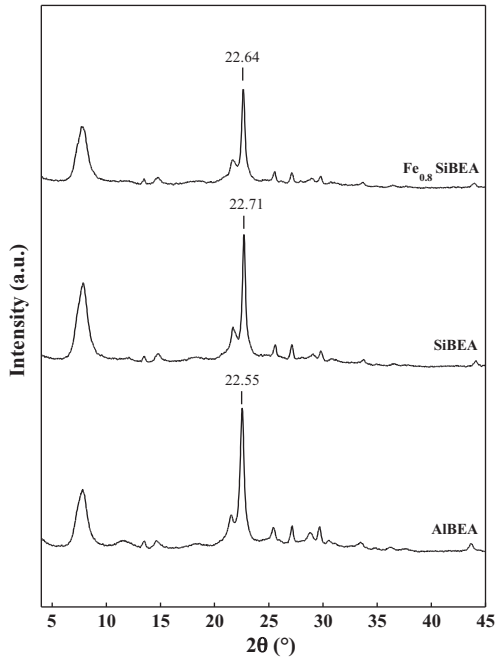

Fig. 1. X-ray diffractograms recorded at room temperature of AlBEA, SiBEA and $Fe_{0.8}$SiBEA as prepared.

3.1.2. Diffuse reflectance UV–vis spectroscopy

Fig. 2 shows the DR UV–vis spectrum of $Fe_{0.8}$SiBEA sample. Two bands at 248 and 274 nm are assigned to oxygen-to-metal charge transfer (CT) transitions involving distorted tetrahedral Fe(III) ions, in line with earlier results [42–47]. The absence of a broad band near 500 nm, suggests that FeO_x oligomers are not present [42–44]. It

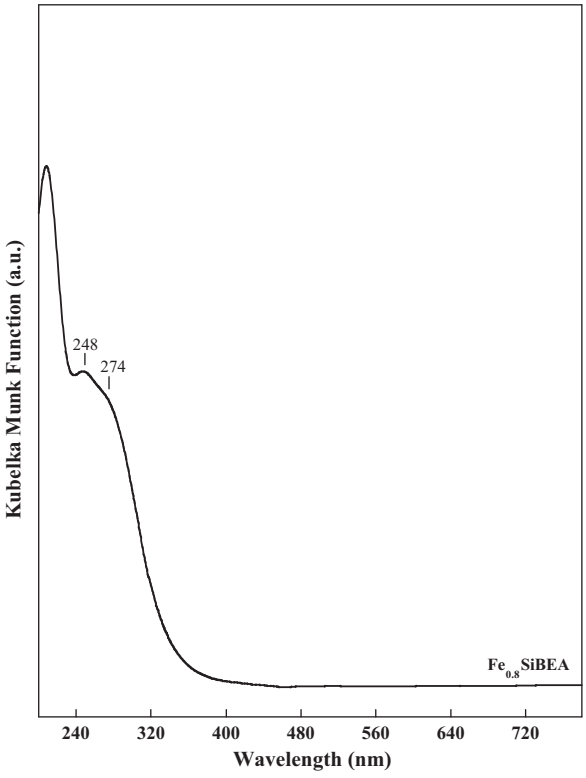

Fig. 2. DR UV–vis spectra recorded at room temperature and ambient atmosphere of $Fe_{0.8}$SiBEA as prepared.

Table 1
Curve fitting results of Fe *K*-edge EXAFS spectra of α-Fe_2O_3, ferrisilicate and $Fe_{0.8}$SiBEA zeolites.

Sample	Shell	C.N.[a]	*R* (Å)[b]	*σ* (Å)[c]	ΔE_0 (eV)	R_f (%)
$Fe_{0.8}$SiBEA	Fe—O	4.9	1.96	0.092	−6.5	10.2
Ferrisilicate	Fe—O	3.8	1.85	0.075	−3.4	9.6
α-Fe_2O_3[d]	Fe—O	3	1.95			
	Fe—O	3	2.11			

ΔE_0 – difference in the origin of photoelectron energy between the reference and the sample (eV), R_f – residual factor (%)
[a] C.N. (±0.6) – coordination number,
[b] *R* (±0.01) – bond length (Å),
[c] *σ* (±0.02) – Debye–Waller factor (Å),
[d] Data on bond length were obtained by X-ray crystallography [50].

suggests that only mononuclear distorted tetrahedral Fe(III) species are present in $Fe_{0.8}$SiBEA zeolite.

3.1.3. EXAFS

Fig. 3 shows k^3-weighted EXAFS spectra and Fourier transforms (not phase shift-corrected) of $Fe_{0.8}$SiBEA sample and ferrisilicate and α-Fe_2O_3 references. The period of oscillations for $Fe_{0.8}$SiBEA is a little shorter than that for ferrisilicate [37], suggesting that they belong to two different types of framework irons in the distorted tetrahedral coordination. The peak at about 1.5 Å can be assigned to the contribution of the Fe—O shell, in line with previous work [48,49]. It should be noted that Fe–Fe interactions detected in α-Fe_2O_3 at about 2.8 Å, are not observed for $Fe_{0.8}$SiBEA and ferrisilicate (Fig. 3) suggesting that iron is isolated and in distorted tetrahedral coordination in both latter cases. However, the higher average coordination number for $Fe_{0.8}$SiBEA (4.9) than for ferrisilicate (3.8) and the larger Fe—O distance for $Fe_{0.8}$SiBEA (1.96 Å) than for ferrisilicate (1.85 Å) (Table 1) suggest that Fe(III) ions belong to two different types of framework ions in the distorted tetrahedral coordination. One of the most reasonable explanations of these results is that Fe(III) of the $Fe_{0.8}$SiBEA and ferrisilicate is located at the different framework positions. These results are in line with earlier reported results of Yan et al. [51] on HZSM-5 with iron impurity and Fe-silicate materials.

3.2. Effect of the type of C_1 and C_2 reducing agents on the catalytic activity of FeSiBEA

In all cases the methane (CH_4) and methanol (MeOH) were chosen as the representatives of C_1 reducing agents and ethylene (C_2H_4) and ethanol (EtOH) as representatives of C_2 reducing agents in the SCR of NO process.

As shown earlier [49], SiBEA is poorly active in SCR of NO by ethanol, with NO conversion below 10% in the 520–775 K range and very low yield of N_2. We have checked (results not shown) that SiBEA is also not active in SCR of NO with methanol, methane and ethylene. These results confirmed that the presence of transition metal ions in the zeolite promote the activity in this process.

The temperature dependence of these organic molecules (methane, methanol, ethylene and ethanol) conversion on $Fe_{0.8}$SiBEA catalyst was shown in Fig. 4. The appropriate curves reflect the reactivity of the organic compounds in SCR reaction. The curves show that the conversion of ethanol and methanol is comparable in large temperature range (525–775 K) and 100% conversion level is attained about 600 K. In the case of ethylene 100% conversion happens at 750 K only. Methane oxidation is very low in the whole temperature range and reaches a value of about 20% at 750 K.

In Fig. 5, the NO conversion is presented in the same reaction temperature range. In this case the superiority of C_2 reagents is clearly visible, at least at reaction temperatures below 673 K, where

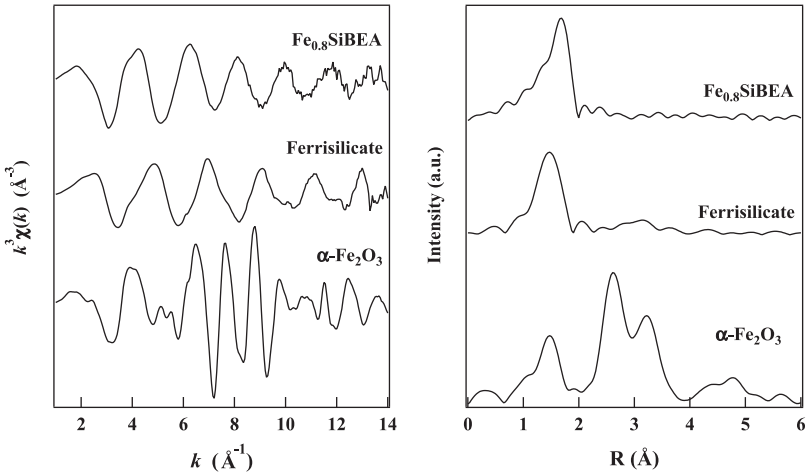

Fig. 3. k^3-weighted EXAFS spectra and Fourier transforms (FTs) recorded at room temperature of α-Fe_2O_3 and ferrisilicate references and $Fe_{0.8}$SiBEA as prepared.

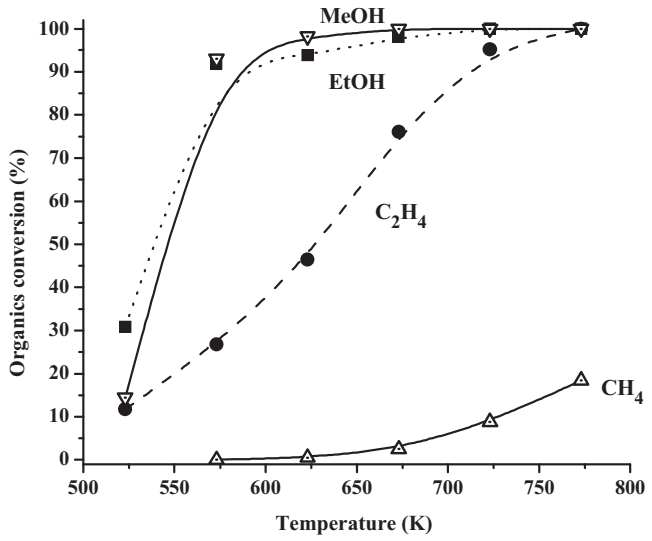

Fig. 4. The temperature dependence of C_1 and C_2 reducing agents conversion in the SCR of NO on $Fe_{0.8}$SiBEA.

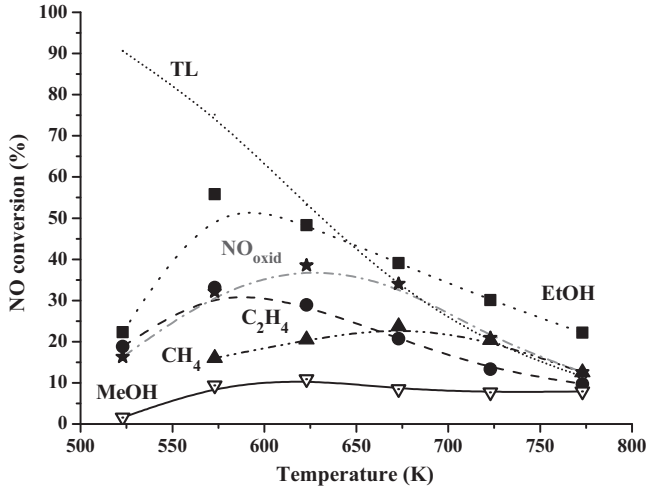

Fig. 5. The temperature dependence of NO conversion in the SCR of NO on $Fe_{0.8}$SiBEA. The dotted line marked as TL represents the thermodynamic limit for reaction (1).

NO conversion in the case of CH_4-SCR becomes superior over C_2H_4-SCR. A very low NO conversion (<10%) in the case of MeOH-SCR in the whole temperature range is more striking. In all cases, the NO conversion graph expresses the volcano-like shape, characteristic for the SCR reactions and at the high end of reaction temperature range NO conversion seems to be limited by the thermodynamic equilibrium reaction:

$$NO + \frac{1}{2}O_2 \rightleftarrows NO_2 \quad (1)$$

It would be expected in the situation when the rate of oxidation reaction of organic molecules is so high, that their concentration approaches nil. The dotted line marked as TL in Fig. 5 represents the thermodynamic limit associated with the reaction (1). Such behaviour evidently takes place for oxidation of NO without organic reagents in the initial reaction mixture (line with asterisks marked in Fig. 5) and, to less extent, for SCR with ethylene. Somewhat peculiar situation occurs in the case of ethanol because NO conversion is higher in the presence of this reducing agent than in the NO oxidation reaction and is also higher than thermodynamic permissible values from 650 K. These results allow us to conclude that NO oxidation to NO_2 and selective catalytic reduction of NO with ethanol into N_2 are competitive but not sequential as it is often suggested in the literature.

This behaviour was also characteristic for other FeSiBEA catalysts with low Fe content [37] and for CoSiBEA catalysts [52]. The lack of correlation between the activity in NO oxidation to NO_2 (Eq. (1)) and SCR of NO with ethanol (Eq. (2)) suggests that the two reactions are more competitive than sequential, and the ratio of N_2/NO_2 depends on the rate constants of both reactions and on the reaction temperature.

$$2NO + 2O_2 + C_2H_5OH \rightarrow N_2 + 2CO_2 + 3H_2O \quad (2)$$

It is likely that the reaction mechanism of SCR of NO with ethanol involves the preliminary adsorption of NO that is oxidized by O_2 forming an adsorbed NO_x species (where $x = 2,3$) bound to framework Fe(III) site, in agreement with our previous work [37]. This site present in $Fe_{0.8}$SiBEA zeolite could activate ethanol molecule by removal hydrogen during the adsorption step and then forming an oxygenated intermediate. This active intermediate is probably responsible for SCR of NO towards N_2.

In other words, the surface (NO_x) species formed in the stage of NO adsorption can react with the oxygenated intermediate leading to formation of N_2. This reaction is in competition with NO_2 desorption. Thus, the appearance of NO_2 in the product do not prove that NO_2 play a role in SCR of NO towards N_2 on FeSiBEA.

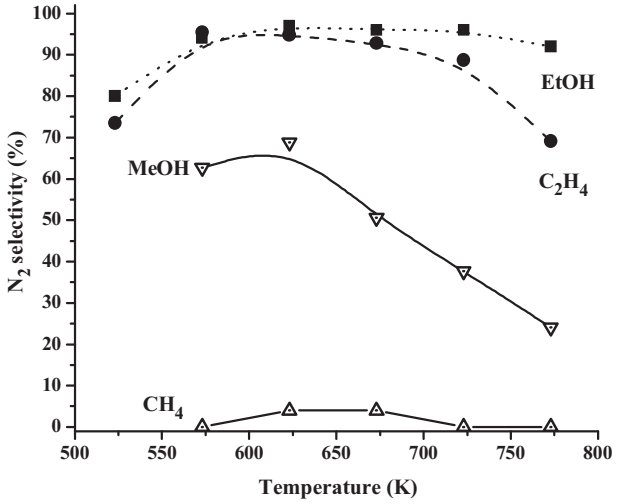

Fig. 6. The temperature dependence of N_2 selectivity in SCR of NO on $Fe_{0.8}$SiBEA.

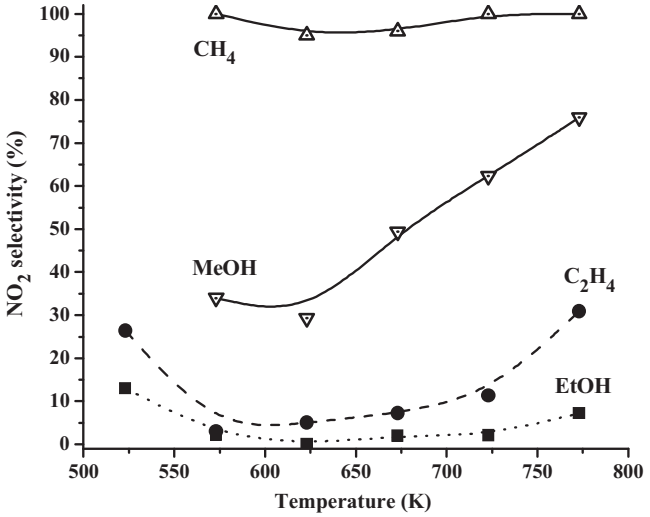

Fig. 7. The temperature dependence of NO_2 selectivity in SCR of NO on $Fe_{0.8}$SiBEA.

This conclusion was additionally confirmed by the results of dependence of the SCR of NO with ethanol activity and selectivity on oxygen partial pressure at 623 K on FeSiBEA catalysts in our earlier report [37], where it was stated that NO conversion is highest for very low oxygen concentration (0.82 vol.% in He) and gradually decreases with increase in oxygen concentration (from 0.82 to 7.5 vol.% in He).

The lower concentration of NO at the reactor outlet at the highest reaction temperatures than that predicted from the thermodynamic calculation suggests that in reaction products some other nitrogen oxides are present, as for example N_2O. It is probable that, despite lack of organic compounds on reactor outlet, some strong adsorbed intermediates being exhausted along the catalyst bed layer participate in SCR process influencing the NO conversion level.

SCR of NO with methane obeys the thermodynamic limitation for NO conversion as well, although in this case the conversion of CH_4 is very low in the whole reaction temperatures range. In contrast to the methane, NO conversion with methanol is very low and never attains the thermodynamic limit, even when the concentration of organics turns to nil at the high reaction temperatures. It indicates that for both C_1 reducing agents the NO conversion level does not reflect the SCR process alone.

Such assumption is fully confirmed in Figs. 6 and 7 where the temperature dependence of N_2 and NO_2 selectivities for all reducing agents is sketched. Indeed, in the case of C_2 reducing agents the N_2 selectivity is very high, exceeding 90% in the range 573–723 K, and NO_2 selectivity is very low in these temperatures. In the same time, N_2 selectivity in CH_4-SCR process is practically negligible and the NO conversion reflects in this case the oxidative power of the FeSiBEA sample. For methanol the situation is more complicated, the lower NO conversion level than that found for CH_4 (Fig. 5) indicates that the oxidation of NO is partially suppressed and its reduction to N_2 occurs with the low rate.

The presented results lead us to the conclusion that the mechanism of the SCR process with C_1 and C_2 reducing agents differs, apart from the fact that both take place on the same reaction centre. It seems that low activity in CH_4-SCR of NO on $Fe_{0.8}$SiBEA catalyst containing only isolated mononuclear distorted tetrahedral Fe(III) species in the framework zeolite (Figs. 2 and 3) can be explained by high energy of C—H bond, which should be broken to activate methane molecule. Indeed, Cant et al. [53] have been recently evidenced on the basis of isotopic effect in the reaction of CH_4 and CD_4 with NO, that the limited step of SCR of NO process on Co-ZSM-5 was dissociative adsorption of methane leading to breaking of C—H bond.

It seems that the SCR of NO into N_2 and NO oxidation into NO_2 seem to be competitive reactions and the ratio of N_2/NO_2 depends on the rate constants of both reactions and on reaction temperature. If we assume that at low temperature, reaction rate between adsorbed (NO_x) species and the reducing agent or desorption of reaction product is the rate determining step, the secondary reaction between NO_2 and adsorbed organic species has no effect on the overall kinetics but the N_2/NO_2 ratio depends on the kind of Fe(III) species present in Fe_xSiBEA zeolites. In the presence of isolated Fe site, as in our case, SCR of NO towards N_2 mainly takes place in the presence of ethanol as shown in Fig. 6. In contrast, when extra framework octahedral Fe species or FeO_x oligomer was present in the Fe_xSiBEA zeolites NO was mainly oxidised into NO_2, as we have reported earlier [37]. The extra framework FeO_x oligomer enhanced the oxidative activity of Fe_xSiBEA converting ethanol to CO_2 and NO to NO_2, in particular at high temperature, at which the concentration of reducing agents is much lower. Such catalytic behaviour of FeO_x oligomers and, especially α-Fe_2O_3-like structure was reported by Kumar et al. for SCR of NO by isobutane or ammonia on Fe-ZSM-5 [54]. Indeed, the presence of the iron oxide phase is detrimental to the SCR activity and causes nonselective oxidation of the reductant (isobutane and ammonia) at higher temperature.

Recently, we have found (results not shown), that catalytic activity of $Fe_{0.8}$SiBEA in nitromethane and nitroethane oxidation and in SCR of NO with these molecules used as reducing agents is very similar, in contrast to strike difference in C_1 and C_2 alcohols activity in SCR of NO process. It suggests that a different effect of C_1 and C_2 alcohols on SCR of NO process is related to the initial step of formation of organic intermediates appeared before reduction of NO towards N2 [55–57]. As evidenced earlier by Erkfeldt et al. [58] the presence of C—C bond in reducing agents is required for their high activity in SCR of NO on Cu-ZSM-5 catalyst. It seems that a C—C bond in the reducing agent is required for SCR of NO process over $Fe_{0.8}$SiBEA. This would also explain why methane and methanol are not active in NO_x reduction as has been shown earlier in other investigations [8,10].

Moreover, it is probable that surface enolic species which could be formed upon partial oxidation of ethanol molecule over FeSiBEA, play an important role as intermediate species in the formation of isocyanate species (—NCO), as it was postulated earlier by Yu et al. [59] on Ag/Al_2O_3. The formation of —NCO species and its effective reaction with $NO + O_2$ seems to be a key step in the SCR of NO

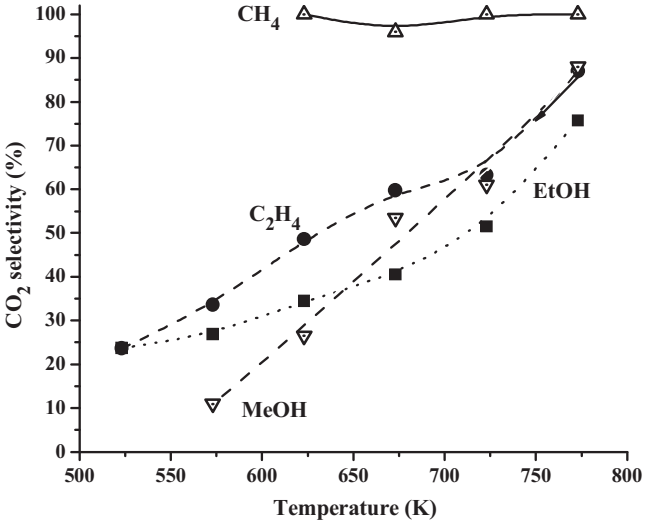

Fig. 8. The temperature dependence of CO_2 selectivity in SCR of NO on $Fe_{0.8}$SiBEA.

process with ethanol. Enolic and —NCO species are not formed when methanol is used as reducing agent what could be a reason of its much lower activity in the SCR process on FeSiBEA catalyst.

In the same time, the striking difference in conversion level of investigated reducing agents is in line with the strength of the weakest bond in the molecules, which is supposed to break in the dissociative adsorption step, but it is not reflected in the activity in SCR of NO process. This is clearly visible comparing organic molecule conversion and SCR activity of CH_3OH and CH_4 (Figs. 3 and 4). As we can see (Fig. 3), methanol very active in oxidation reaction is not effective reducing agent in SCR of NO (Fig. 4).

The additional information concerning the C_1- and C_2-SCR process can be issued from the analysis of the Fig. 8. It is seen, that with the exception of CH_4, in all cases oxidation of organic molecules is not selective, and a lot of organic intermediates, mainly CO, and then aldehydes, organic acids, ethers and small amounts of acetonitrile (results not shown) are produced when ethanol is used as reducing agent. It explains the high level of NO conversion in the case of EtOH-SCR, but confirms the statement that the presence of organic "active" intermediates is not sufficient condition for the high NO reduction level.

Finally, it should be stressed that at least for EtOH- and MeOH-SCR of NO process, the reducing agents conversion is independent of the presence of NO_2 in the reaction zone (not published results), what confirms assumption that NO_x adsorbed species does not hinder the rate of reducing agents adsorption.

4. Conclusions

FeSiBEA zeolite with 0.8 Fe wt% prepared in acidic conditions (pH 2.5) by a two-step postsynthesis method allows to control the incorporation of iron into framework of BEA zeolite evidenced by XRD.

For such low Fe content, iron is incorporated into the zeolite as mononuclear framework tetrahedral Fe(III) species as evidenced by DR UV–vis and EXAFS spectroscopies.

The single site FeSiBEA catalyst with isolated and framework Fe centres are active in SCR of NO process with C_2 (ethanol and ethylene) reducing agents, with selectivity towards N_2 exceeding 90% in the broad temperature range (573–723 K).

The single site FeSiBEA catalyst is much less active in SCR of NO with C_1 (methanol and methane) reducing agents with selectivity towards N_2 not exceeding 65% with methanol and only 10% with methane.

The formation of —NCO species and its effective reaction with $NO + O_2$ seems to be a key step in the SCR of NO process with ethanol. It is probable that absence of formation of enolic and —NCO species when methanol is used as reducing agent is a reason of much lower activity of FeSiBEA catalyst in the SCR process.

Further studies are underway to explain the different behaviour of single site FeSiBEA catalyst in SCR of NO with ethanol and methanol as reducing agents.

References

[1] M.D. Uddin, T. Komatsu, T. Kashima, Journal of Catalysis 150 (1994) 439.
[2] P.B. Venuto, Microporous Materials 2 (1994) 297.
[3] K.A. Dubkov, V.I. Sibolev, G.I. Panov, Kinetics and Catalysis 39 (1998) 72.
[4] X. Feng, W.K. Hall, Catalysis Letters 41 (1996) 45.
[5] H.Y. Chen, W.M.H. Sachtler, Catalysis Today 42 (1998) 73.
[6] G. Centi, F. Vazanna, Catalysis Today 53 (1999) 683.
[7] A.Z. Ma, W. Grünert, Journal of the Chemical Society, Chemical Communications (1999) 71.
[8] R. Burch, S. Scire, Applied Catalysis B 3 (1994) 295.
[9] T. Beutel, Z. Zhang, W.M.H. Sachtler, H. Knözinger, Journal of Physical Chemistry 97 (1993) 3579.
[10] Y. Li, J.N. Armor, Applied Catalysis B 2 (1993) 239.
[11] M. Haneda, Y. Kintaichi, H. Shimada, H. Hamada, Journal of Catalysis 192 (2000) 137.
[12] M. Haneda, Y. Kintaichi, H. Mizushima, N. Kakuta, H. Hamada, Applied Catalysis B 31 (2001) 81.
[13] S. Dzwigaj, J. Janas, T. Machej, M. Che, Catalysis Today 119 (2007) 133.
[14] T. Tabata, M. Kokitsu, H. Ohtsuka, O. Okada, L.M.F. Sabatino, G. Bellussi, Catalysis Today 27 (1996) 91.
[15] H. Ohtsuka, T. Tabata, O. Okada, Catalysis Today 42 (1998) 45.
[16] T. Tabata, H. Ohtsuka, L.M.F. Sabatino, G. Bellussi, Microporous Mesoporous Materials 21 (1998) 517.
[17] H.H. Chen, S.C. Shen, X. Chen, S. Kawi, Applied Catalysis B 50 (2004) 37.
[18] B. Wichterlova, Z. Sobalik, J. Dedecek, Applied Catalysis B 41 (2003) 97.
[19] Y. Traa, B. Burger, J. Weitkamp, Microporous Mesoporous Materials 30 (1999) 3.
[20] G. Bagnasco, M. Turco, C. Resini, T. Montanari, M. Bevilacqua, G. Busca, Journal of Catalysis 225 (2004) 536.
[21] J. Janas, T. Machej, J. Gurgul, L.P. Socha, M. Che, S. Dzwigaj, Applied Catalysis B 75 (2007) 239.
[22] F. Kapteijn, G. Marban, I. Rodriguez-Mirasol, J.A. Moulijn, Journal of Catalysis 167 (1997) 256.
[23] E.M. El-Malki, R.A. van Santen, W.M.H. Sachtler, Journal of Catalysis 196 (2000) 212.
[24] F. Kapteijn, J. Rodrigues-Mirasol, J.A. Moulijn, Applied Catalysis B 9 (1996) 25.
[25] J.A.Z. Pieterse, S. Booneveld, R.W. van den Brink, Applied Catalysis B 51 (2004) 215.
[26] G.D. Pirngruber, P.K. Roy, Catalysis Today 110 (2005) 199.
[27] G.D. Pirngruber, P.K. Roy, Catalysis Letters 93 (2004) 75.
[28] M. Kogel, R. Monnig, W. Schwieger, A. Tissler, T. Turek, Journal of Catalysis 182 (1999) 470.
[29] J. Jia, K.S. Pillai, W.M.H. Sachtler, Journal of Catalysis 221 (2004) 119.
[30] A. Ribera, I.W.C.E. Arends, S. De Vries, J.P. Sheldon, Journal of Catalysis 195 (2000) 287.
[31] J. Perez-Ramirez, E.V. Kondratenko, Journal of the Chemical Society, Chemical Communications (2003) 2152.
[32] Q. Kan, Z. Wu, R. Xu, X. Liu, S. Peng, Journal of Molecular Catalysis 74 (1992) 223.
[33] M. Iwamoto, H. Yahiro, Y. Yuu, S. Shundo, N. Mizuno, Shokubai 32 (1990) 430.
[34] W. Held, A. König, T. Richter, L. Puppe, Society of Automotive Engineers [Special Publication] SP (1990), SP-810 (Recent Trends Automot. Emiss. Control) 13.
[35] S. Dzwigaj, J. Janas, W. Rojek, L. Stievano, F.E. Wagner, F. Averseng, M. Che, Applied Catalysis B 85 (2009) 45.
[36] S. Dzwigaj, M.J. Peltre, P. Massiani, A. Davidson, M. Che, T. Sen, S. Sivasanker, Chemical Communications 87 (1998).
[37] J. Janas, J. Gurgul, R.P. Socha, T. Shishido, M. Che, S. Dzwigaj, Applied Catalysis B 91 (2009) 113.
[38] J.W. Cook, D.E.J. Sayers, Applied Physics 52 (1981) 5024.
[39] A.L. Ankudinov, B. Ravel, J.J. Rehr, S.D. Conradson, Physical Review B 58 (1998) 7565.
[40] S. Dzwigaj, M. Matsuoka, R. Franck, M. Anpo, M. Che, Journal of Physical Chemistry B 102 (1998) 6309.
[41] M.A. Camblor, A. Corma, J. Pérez-Pariente, Zeolites 13 (1993) 82.
[42] S. Bordiga, R. Buzzoni, F. Geobaldo, C. Lamberti, E. Giamello, A. Zecchina, G. Leofanti, G. Petrini, G. Tozzola, G. Vlaic, Journal of Catalysis 158 (1996) 486.
[43] H.H. Tippins, Physical Review B 72 (1970) 279.
[44] P. Wu, T. Komatsu, T. Yashima, Microporous Mesoporous Materials 20 (1998) 139.
[45] L. Capek, V. Kreibich, J. Dedecek, T. Grygar, B. Wichterlova, Z. Sobalik, J.A. Martens, R. Brosius, V. Tokarova, Microporous Mesoporous Materials 80 (2005) 279.

[46] J. Perez-Ramirez, J.C. Groen, A. Brückner, M.S. Kumar, U. Bentrup, M.N. Debbagh, L.A. Villaescusa, Journal of Catalysis 232 (2005) 318.
[47] M. Schwidder, S. Heikens, A. De Toni, S. Geisler, M. Berndt, A. Brückner, W. Grünert, Journal of Catalysis 259 (2008) 96.
[48] J.H. Choy, J.B. Yoon, D.K. Kim, S.H. Hwang, Inorganic Chemistry 34 (1995) 6524.
[49] T.E. Westre, P. Kennepohl, J.G. de Witt, B. Hedman, K.O. Hodgson, E.I. Solomon, Journal of the American Chemical Society 119 (1997) 6297.
[50] R.W.G. Wyckoff, Crystal Structure, vol. 2, 2nd ed., Interscience Publishers, New York, 1986.
[51] G. Yan, J. Long, X. Wang, Z. Li, X. Wang, Y. Xu, X. Fu, Journal of Physical Chemistry C 111 (2007) 5195.
[52] J. Janas, T. Machej, J. Gurgul, R.P. Socha, M. Che, S. Dzwigaj, Applied Catalysis B 75 (2007) 239.
[53] N.W. Cant, D.C. Chambers, A.D. Cowan, I.O.Y. Liu, A. Satsuma, Topics in Catalysis 10 (2000) 13.
[54] M.S. Kumar, M. Schwidder, W. Grünert, A. Brückner, Journal of Catalysis 227 (2004) 384.
[55] V. Zuzaniuk, F.C. Meunier, J.R.H. Ross, Journal of Catalysis 202 (2001) 340.
[56] S. Kameoka, Y. Ukisu, T. Myiadera, Physical Chemistry Chemical Physics 2 (2000) 367.
[57] S. Tamm, H.H. Ingelsten, A.E.C. Palmquist, Journal of Catalysis 255 (2008) 304.
[58] S. Erkfeldt, A. Palmqvist, M. Petersson, Applied Catalysis B 102 (2011) 547.
[59] Y. Yu, H. He, Q. Feng, H. Gao, X. Yang, Applied Catalysis B 49 (2004) 159.